

Formation and characterization of a new monoclinic lithium manganese oxide: m-type Li_xMnO_2

Frédéric Le Cras,^{a,b} Pierre Strobel,^{*a} Michel Anne^a and Didier Bloch^b

^aLaboratoire de Cristallographie CNRS, BP 166, 38042 Grenoble Cedex 9, France

^bCEA, DEM/SPCM/LSE, 38054 Grenoble Cedex 9, France

A new lithium manganese oxide with formula Li_xMnO_2 ($x=0.2-0.3$), denoted as m-phase, has been identified and isolated. First noticed as an intermediate phase during the early steps of the solid-state synthesis of Li-Mn-O spinels at low temperature, it can be isolated by extended annealing and grinding mixtures of finely divided $\beta\text{-MnO}_2$ and LiOH or Li_2CO_3 at 150 °C. Its X-ray pattern can be indexed as primitive monoclinic with $a=938$, $b=565.5$, $c=490.6$ pm and $\beta=102.2^\circ$. Thermogravimetric and X-ray investigations show that it is stable up to ca. 550 °C. The m-phase structure appears to be rather rigid. It allows only limited lithium extraction in acidic medium and limited electrochemical lithium intercalation, with maximum reversible capacity $\Delta x=0.25$ Li per formula unit. These properties confirm that it is a new oxide, with a rather different behaviour from that of known spinel-type or layered Li-Mn-O compounds.

During a comprehensive study of the low-temperature synthesis of Li-Mn-O spinel oxides using finely divided $\beta\text{-MnO}_2$ as the manganese source a set of unknown reflections was systematically noticed during the first steps of the thermal treatments in the temperature range 200–400 °C.¹ It was realized that (i) this set could not be attributed to any known compound containing the elements Li, Mn, O, as well as H or C, and had to be ascribed to a new, unknown phase; (ii) these reflections disappeared on further annealings at higher temperature. This latter observation probably explains why it was never reported before, since dense precursors such as $\beta\text{-MnO}_2$ were previously thought to be inefficient reagents for low-temperature solid-state reactions. Given the considerable interest of the Li-Mn-O system for positive electrode materials in rechargeable lithium batteries,^{2,3} this new phase was studied in more detail. The present paper describes the preparation conditions of the new compound in single phase form, its structural and thermogravimetric characterization, and its behaviour as host for electrochemical lithium intercalation. This new phase will be referred to as 'm phase' throughout this paper, because it has been found to have monoclinic symmetry.

Experimental

Syntheses were carried out using LiOH·H₂O (Prolabo) or Li_2CO_3 (Merck) and low grain-size $\beta\text{-MnO}_2$ (supplied by Sedema). Reagents were ground and mixed in a planetary mill for 1 h, and heated in a tubular, rotating furnace under oxygen flow.

Lithium and manganese contents were analyzed using atomic absorption analysis on samples dissolved in 2.5 M hydrochloric acid. In some cases, the total manganese content was also determined by potentiometric titration of the manganese(III) phosphate complex in acidic medium. Both methods gave consistent results. The average manganese oxidation state was obtained by permanganate back-titration after reduction of samples dissolved in 2 M sulfuric acid by excess oxalic acid. The estimated accuracy on the analyses was 5 and 2% on atomic absorption and volumetric titration, respectively.

Reaction products were characterized by powder X-ray diffraction on a Siemens D-5000 diffractometer equipped with a diffracted-beam monochromator, rotating sample holder, and operated with Cu-K α radiation. Cell parameters were determined by cell-constrained profile refinements using the

whole pattern fitting method (Fullprof program⁴), on X-ray data acquired with counting time ≥ 60 s per step. Additional structural information was obtained in a Philips CM 300 electron microscope operated at 300 kV.

Thermogravimetry was carried out using an automated Perkin-Elmer TG-7 thermobalance in a constant flow of dried oxygen, with a 30 °C h⁻¹ heating/cooling regime. Electrochemical intercalation was performed in lithium coin cells, using a LiClO_4 in propylene carbonate-ethylene carbonate-dimethoxyethane electrolyte, and assembled in a glove box under argon, as described previously.⁵

Results and Discussion

Conditions for m-phase formation

Fig. 1 shows an example of emergence and disappearance of phase m during the first stages of $\text{Li}_{1+x}\text{Mn}_{2-x}\text{O}_4$ spinel formation at 200 °C from a $\beta\text{-MnO}_2\text{-Li}_2\text{CO}_3$ mixture with cationic ratio Li/Mn=0.80 ($x=1/3$). The most typical extra reflections occur at 15.6, 18.5 (shoulder on the 111 spinel reflection), 19.4 and 22.6° 2 θ (Cu) (see white arrows in Fig. 1).

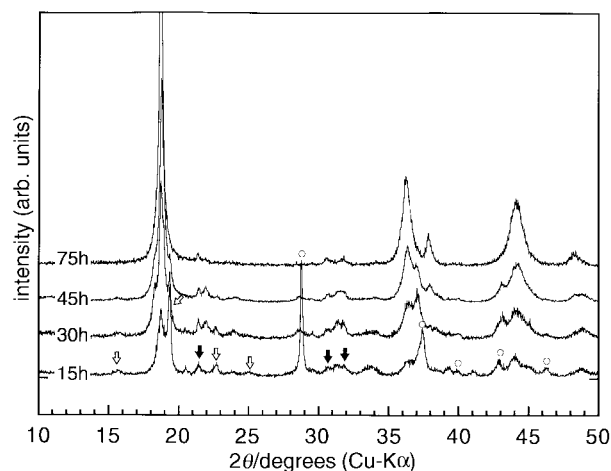


Fig. 1 Evolution of the X-ray diffraction pattern of a $\text{Li}_{0.8}\text{MnO}_x$ sample treated at 200 °C as a function of annealing time. Non-spinel phases detected: white dots, $\beta\text{-MnO}_2$; black arrows, Li_2CO_3 ; white arrows, unknown phase.

The new phase is most prominent at temperatures $\leq 200^\circ\text{C}$. Its formation was studied in more detail at 150°C , where we followed the evolution of a sample heated for repeated periods of 5 h with systematic X-ray examination and regrinding (2 h ball-milling) between successive heatings. As shown by X-ray diffraction (Fig. 2), the last traces of $\beta\text{-MnO}_2$ disappear after *ca.* 240 h heating treatment. More remarkable is the absence of spinel phase formation. The only remaining impurity on longer annealing is lithium carbonate.

The new phase has also been subjected to an acidic treatment with 0.1 M HNO_3 at room temperature. This reaction was carried out with a double objective: (i) attempting to eliminate the residual lithium carbonate, (ii) checking whether or not the new m phase can give rise to oxidative lithium extraction such as that observed in the spinel phase in such conditions.⁶



Physico-chemical characterization

The determinations of total manganese and oxidative power in the final sample N (reacted at 150°C for 7 weeks) yielded an average oxidation state $\nu(\text{Mn})=3.76$. Although stoichiometric MnO_2 is thermodynamically stable under 1 atm oxygen up to *ca.* 500°C ,⁷ the oxidation state in the mixture in the presence of a lithium reagent drops, even in oxygen atmosphere. Taking into account the initial molar ratio, the analytical data give for sample N a composition close to $\text{Li}_{0.31}\text{MnO}_{2.03} + 0.25\text{Li}_2\text{CO}_3$.

A treatment in excess 0.1 M nitric acid at room temperature for 4 h has the following effects: (i) the disappearance of all lithium carbonate reflections in the X-ray powder pattern (see Fig. 3), (ii) a decrease in Li/Mn ratio from 0.31 to $0.22 (\pm 0.02)$ from atomic absorption analysis, (iii) a surprisingly negligible change in manganese oxidation state (measured values 3.76 and 3.75 before and after acid treatment, respectively), as well as in the position of the m phase X-ray reflections. The formula after washing out the remaining lithium carbonate is thus $\text{Li}_{0.22}\text{MnO}_{1.985}$, and this treatment shows that the m-phase structural network is much less flexible than the spinel one regarding mobility and extraction of Li^+ ions from the struc-

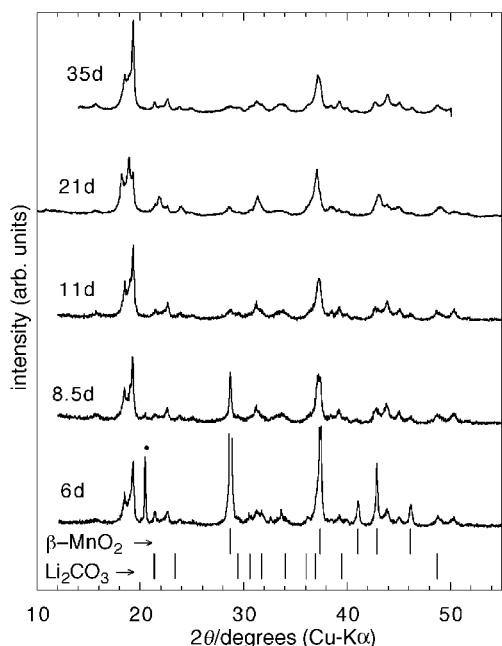


Fig. 2 Same as Fig. 1 at 150°C . The dot at 20.5° indicates the strongest LiOH reflection. Annealing durations (in days) are indicated.

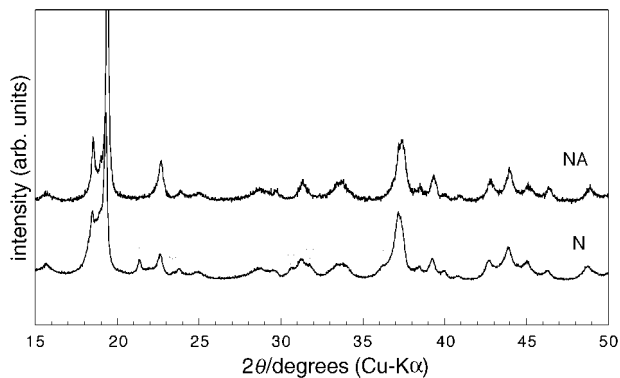


Fig. 3 Comparison of X-ray diffraction diagrams of samples N and NA (before and after nitric acid treatment, respectively). The strongest Li_2CO_3 reflections are indicated by arrows.

ture. Taking into account the experimental uncertainties, the formula of the acid-treated will be written hereafter $\text{Li}_{0.22}\text{MnO}_2$.

Structural characterization

The unit cell of the new phase was determined using the automatic indexing program Treor 90.⁸ The whole set of observed reflections can be indexed in a primitive monoclinic cell ($P2$, Pm or $P2/m$). Cell constrained profile refinements (see Fig. 4) yielded the cell parameters values given in Table 1. A listing of observed and calculated d -spacings and intensities is given in Table 2.

Such a cell shows no isotopy with any known manganese oxide. Several features deserve to be pointed out:

$b/2 = 283$ pm, which is the characteristic length of $\text{Mn}(+4)\text{O}_6$ octahedra edges in structures built up of corner- or edge-sharing MnO_6 octahedra: $\beta\text{-MnO}_2$ (rutile structure), ramsdellite, hollandite and phyllo-manganates(+4) all have MnO_6 octahedra edges in the range 282–287 pm.^{9,10}

$c/b \approx \sqrt{3}/2$, showing a pseudo-hexagonal subcell. This feature has been confirmed by electron diffraction (see Fig. 5).

The $k = 2n + 1$ reflections are markedly broader than other reflections, showing possible hints of superstructure with a basic subcell based on $b/2 = 283$ pm. All these features are consistent with the presence of octahedral MnO_6 units in the structure. The three-dimensional connectivity of these octahedra, however, seems to differ from that in other known manganese oxides.

Thermogravimetry

The thermal stability of acid-treated m phase in oxygen atmosphere has been investigated by thermogravimetry, and

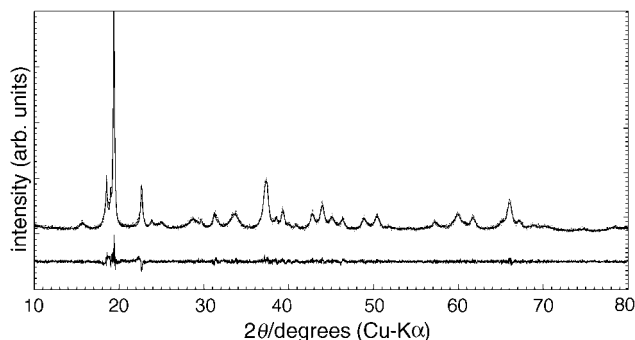


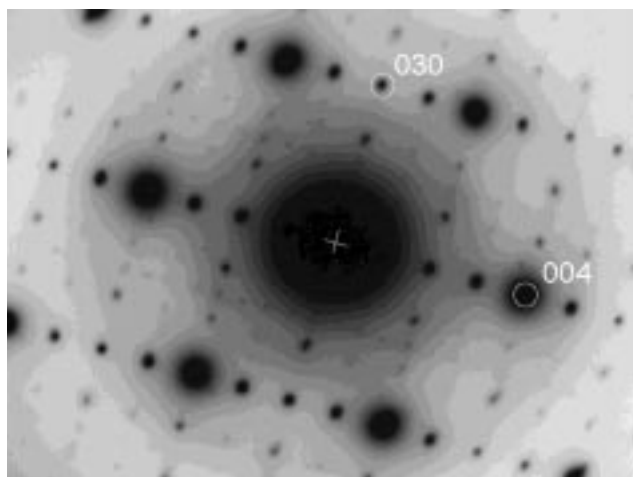
Fig. 4 Result of the full X-ray pattern-matching profile refinement (program Fullprof⁴) for $\text{Li}_{0.22}\text{MnO}_2$ (sample NA, acid-treated to remove lithium carbonate). The linewidths of reflections with k odd and even have been refined independently.

Table 1 Refined cell parameters on various m-phase samples

sample	$a/\text{\AA}$	$b/\text{\AA}$	$c/\text{\AA}$	$\beta/^\circ$	$V/\text{\AA}^3$	R_p	R_{wp}	R_{exp}	χ^2
M (120 h)	9.418(4)	5.656(2)	4.915(1)	102.14(2)	256.01	6.58	8.79	4.00	4.84
NA (acid-treated)	9.380(2)	5.655(1)	4.906(1)	102.17(2)	254.43	10.1	13.1	10.23	1.64
NT (340 °C)	9.376(1)	5.654(1)	4.903(1)	102.30(1)	253.93	6.35	8.17	5.58	2.15

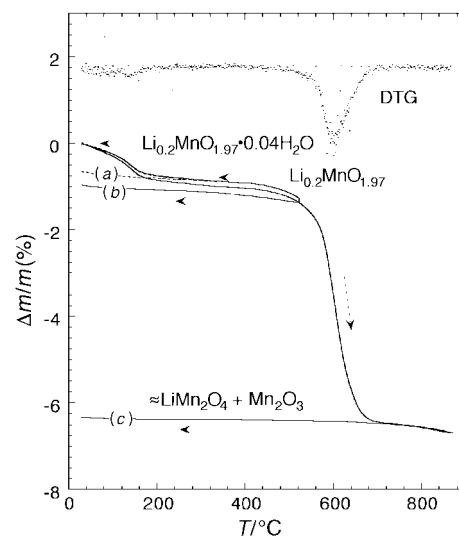
Table 2 Listing of observed and calculated reflections of m-phase $\text{Li}_{0.3}\text{MnO}_2$ (reflections with $I < 2$ have been neglected)

h	k	l	I	d_{obs}	d_{calc}	$2\theta_{(Cu)}$	h	k	l	I	d_{obs}	d_{calc}	$2\theta_{(Cu)}$
0	1	0	9	5.656	5.655	15.657	3	1	-2	7	—	1.981	45.752
1	1	0	26	4.788	4.813	18.417	2	0	2	6	1.957	1.962	46.238
0	0	1	9	—	4.796	18.485	4	0	-2	9	1.863	1.865	48.788
1	0	-1	10	4.666	4.673	18.973	4	1	1	8	—	1.816	50.208
2	0	0	100	4.575	4.585	19.343	3	2	1	9	1.810	1.813	50.295
1	0	1	26	3.920	3.924	22.644	4	2	-1	2	1.765	1.766	51.706
2	0	-1	3	3.728	3.730	23.835	2	2	2	6	1.609	1.612	57.096
0	1	1	3	—	3.658	24.315	4	2	1	2	—	1.587	58.083
2	1	0	7	3.565	3.562	24.981	2	1	-3	2	—	1.557	59.313
2	1	-1	13	3.110	3.114	28.645	5	2	-1	7	—	1.547	59.730
2	0	1	4	3.005	3.012	29.634	5	1	1	6	1.543	1.543	59.892
3	0	-1	11	2.856	2.866	31.182	5	2	0	2	—	1.539	60.080
0	2	0	5	2.825	2.828	31.617	6	0	0	3	—	1.528	60.529
3	1	0	15	2.682	2.689	33.291	1	0	3	3	—	1.522	60.830
2	1	1	19	2.656	2.658	33.685	4	0	2	7	—	1.506	61.522
1	0	-2	6	—	2.450	36.654	3	1	-3	6	1.502	1.502	61.711
1	2	-1	22	2.413	2.419	37.133	4	3	-1	2	—	1.448	64.268
2	2	0	19	2.404	2.407	37.333	1	3	2	7	—	1.434	64.990
0	0	2	11	—	2.398	37.475	2	0	3	7	—	1.419	65.737
3	0	1	3	2.354	2.362	38.069	4	1	-3	6	—	1.417	65.841
2	0	-2	6	2.337	2.337	38.494	1	2	-3	9	—	1.415	65.969
1	2	1	13	2.291	2.294	39.242	0	4	0	8	1.414	1.414	66.029
4	0	0	2	—	2.293	39.266	5	2	-2	2	1.414	1.414	66.036
2	2	-1	2	2.253	2.253	39.979	1	4	0	4	—	1.397	66.911
3	0	-2	12	2.116	2.116	42.703	5	2	1	4	1.394	1.395	67.027
4	1	-1	5	—	2.100	43.028	3	2	-3	4	1.365	1.364	68.740
2	2	1	16	2.059	2.062	43.882	0	4	2	4	1.217	1.218	78.469
1	1	2	12	—	2.057	43.975	3	0	-4	4	1.203	1.206	79.398
3	2	-1	9	2.012	2.013	45.000							

**Fig. 5** Electron diffraction pattern of $\text{Li}_{0.3}\text{MnO}_2$ (sample N) ([100] zone)

by X-ray diffraction after annealings at 340, 525 and 870 °C followed by slow cooling.

The thermogravimetric behaviour of acid-treated $\text{Li}_{0.22}\text{MnO}_2$ (see Fig. 6) shows the occurrence of two mass losses: (i) a small (0.8%) mass loss at temperature ≤ 150 °C, attributable to the departure of adsorbed water, (ii) a much larger (6.1%) and irreversible loss with maximum kinetics at 605 °C. The latter corresponds to the departure of oxygen accompanying the decomposition of the m phase into products with lower manganese oxidation state. The X-ray powder diffraction pattern of the decomposition products after heating

**Fig. 6** TG and DTG curves of acid-treated $\text{Li}_{0.22}\text{MnO}_2$ in oxygen up to 340 °C (a), 525 °C (b) and 870 °C (c)

at 870 °C shows the presence of a mixture of spinel and dimanganese trioxide. A refinement of these X-ray data using the Rietveld method yielded a composition $\text{Li}_{1.03}\text{Mn}_{1.97}\text{O}_4$ (spinel structure, $a = 8.238$ Å, 58 mass%) + $\alpha\text{-Mn}_2\text{O}_3$ (42 mass%).

Note that this result allows one to calculate indirectly the composition of the m phase, knowing the mass loss resulting in the spinel– Mn_2O_3 mixture. Such a calculation yields the

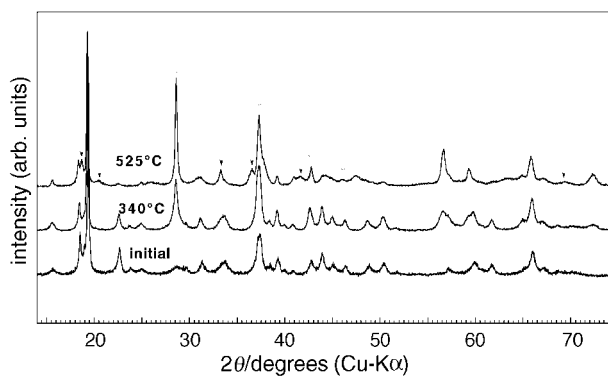
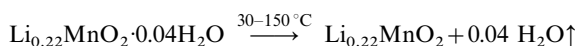


Fig. 7 Effect of 340 and 525 °C oxygen-annealing on the X-ray diffraction pattern of acid-treated $\text{Li}_{0.22}\text{MnO}_2$. Black and white arrows show reflections of Li_2MnO_3 and $\beta\text{-MnO}_2$, respectively.

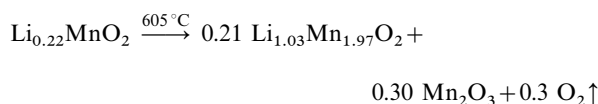
formula $\text{Li}_{0.195}\text{MnO}_{1.973}$, in good agreement with the chemical determination for the acid-treated phase (*vide supra*).

X-Ray and mass loss data are consistent with the following reactions:

step (i):



step (ii):



Additional X-ray data after annealing at intermediate temperatures (see Fig. 7) show that the m phase is stable at least up to 525 °C. After annealing at 340 °C, one observes a sharpening of the m phase reflections, but also the appearance of $\beta\text{-MnO}_2$ (and possibly of Li_2MnO_3 , difficult to detect because of reflection overlapping). At 525 °C, this reaction is enhanced and Li_2MnO_3 is clearly visible. Most m-phase reflections are attenuated, but the m phase is still present (see typical reflections at 2θ 15.6, 18.4, 19.3 and 66.0° in Fig. 7). A comparison of the m phase/ $\beta\text{-MnO}_2$ peak intensity ratios with those in sample D (see Fig. 2) shows that the amount of $\beta\text{-MnO}_2$ formed at 525 °C is small. This partial decomposition step is not noticeable by thermogravimetry since both $\beta\text{-MnO}_2$ and Li_2MnO_3 contain tetravalent manganese, so that no oxygen loss is required for this reaction. In any case, these experiments show that the m phase has a larger thermal stability than the acid-treated spinel $\lambda\text{-MnO}_2$, which is transformed into $\beta\text{-MnO}_2$ at 258 °C in oxygen,⁶ or lithium phyllosilicate, which becomes heavily disordered when heated above 400 °C.¹¹

Electrochemical behaviour

The behaviour of phase m as a cathode in lithium cells has been investigated using the electrochemical voltage spectroscopy technique (EVS) at 12.5 mV h^{-1} . The results (Fig. 8) show a very broad current peak centered at 2.75 V in discharging and at ca. 3.10 V in charging. At high potentials, a weak oxidation wave begins above 4 V. It is not observed on discharge and is clearly dominated by partial oxidation of the electrolyte (ethylene carbonate–dimethoxyethane). This behaviour seems to be rather stable and reversible (see cycle numbers on Fig. 8). However, the resulting intercalation capacity does not exceed 0.25 Li per formula unit, *i.e.* 77 mA h g^{-1} (see Fig. 9).

This behaviour differs widely from that of spinels $\text{Li}_{1+x}\text{Mn}_{2-x}\text{O}_4$, regarding both the exchanged capacities and the shape of the EVS curves. For phase m, the observed redox intercalation is smeared over a much wider potential range than in spinels, while the capacity is smaller. The broadness of

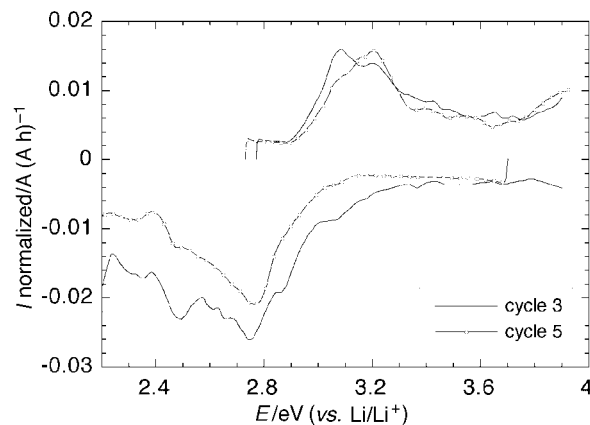


Fig. 8 Potentiostatic behaviour of m-type $\text{Li}_{0.22}\text{MnO}_2$ in a lithium cell (cell 125, liquid electrolyte, active mass 19.60 mg, potential stepping speed 12.5 mV h^{-1})

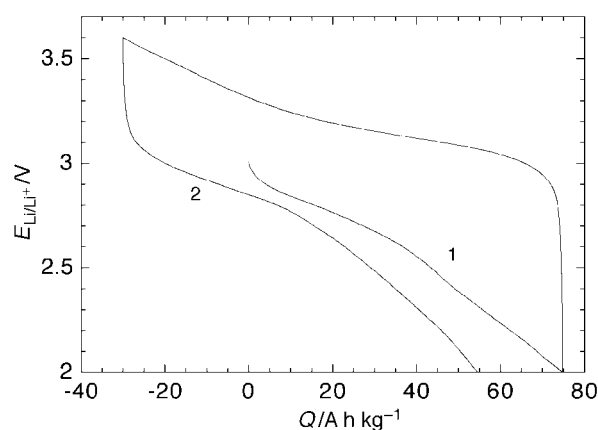


Fig. 9 Evolution of the potential as a function of lithium intercalation in the m phase (same conditions as in Fig. 8)

the current peaks, as well as the overlap between oxidation and reduction waves, point to a single-phase reaction, in contrast with the spinel case, where the intercalation occurs at a well defined potential corresponding to a two-phase equilibrium between a cubic initial phase and a tetragonal intercalated one.² This phase transition is due to the Jahn–Teller effect induced by the important fraction of Mn^{3+} ions (with electronic configuration d^4) in the intercalated material, especially when starting from a spinel phase with $\alpha=0$ [initial oxidation state $v(\text{Mn}) = +3.5$].

On the contrary, the intercalation reaction in the m phase seems to stop at this very oxidation state [initial $v(\text{Mn}) = +3.75$, $\Delta v(\text{Mn})$ on intercalation = 0.25]. The limited capacity observed could thus be due to the inability of the m-phase structure to accommodate heavily distorted MnO_6 octahedra such as those found in tetrahedrally distorted spinels (hausmannite structure). An examination of the positive electrode pellet from an electrochemical cell discharged to 2.2 V shows a complex X-ray diagram, with broadened m-phase reflections combined with those of other constituents (PTFE binder, carbon), without any evolution towards a spinel structure. This result confirms the specificity of the m-type structure, which appears to be rather rigid. Its electrochemical behaviour differs from that of spinels, as discussed above, and also from that of layered Li_xMnO_2 ('phyllosilicates'),^{12,13} the structure of which is more flexible, but also more fragile, and is progressively converted into spinel for dehydrated materials.¹²

Conclusions

We have shown that the Li–Mn–O system forms a new oxide at low temperature, with formula Li_xMnO_2 ($x = 0.2\text{--}0.3$). The X-ray diffraction pattern is indexable in a primitive monoclinic cell, and shows evidence of a hexagonal subcell with a axis typical of octahedrally coordinated tetravalent manganese. Its thermal stability and limited ability in reversible lithium intercalation capacity show that this new structural arrangement is rather rigid. Further work is in progress concerning the structure of this new monoclinic oxide.

F. Le Cras was funded by a BDCI grant partly supplied by Bolloré Technologies, Quimper, France. The authors also thank L. Pontonnier (CNRS) and D. Tisserand for her assistance in electron diffraction and atomic absorption experiments.

References

- 1 D. Bloch, F. Le Cras and P. Strobel, *J. Power Sources*, 1996, **63**, 71.
- 2 M. M. Thackeray, *Prog. Batt. Batt. Mater.*, 1992, **11**, 150.

- 3 D. Guyomard and J. M. Tarascon, *Solid State Ionics*, 1994, **69**, 222.
- 4 J. Rodriguez-Carvajal, Institut Laue-Langevin, Grenoble, 1990 and 15th Congress of the IUCr, 1990, 127.
- 5 P. Strobel, S. Rohs and F. Le Cras, *J. Mater. Chem.*, 1996, **6**, 1591.
- 6 J. C. Hunter, *J. Solid State Chem.*, 1981, **39**, 142.
- 7 O. Barin, O. Knacke and O. Kubaschewski, *Thermochemical Properties of Inorganic Substances*, Springer, Berlin, 1973–1977.
- 8 P. E. Werner, L. Eriksson and M. Westdahl, *J. Appl. Crystallogr.*, 1985, **18**, 367.
- 9 R. Giovanoli and E. Staehli, *Chimia*, 1970, **24**, 49.
- 10 P. Strobel and J. C. Charenton, *Rev. Chim. Miner.*, 1986, **23**, 125.
- 11 P. Strobel, F. Le Cras, S. Rohs and L. Pontonnier, *Mater. Res. Bull.*, 1996, **31**, 1417.
- 12 F. Le Cras, S. Rohs, M. Anne and P. Strobel, *J. Power Sources*, 1995, **54**, 319.
- 13 P. Le Goff, N. Baffier, S. Bach and J. P. Pereira-Ramos, *J. Mater. Chem.*, 1994, **4**, 133; 875.

Paper 7/04377E; Received 23rd June, 1997